AIAA JOURNAL
Vol. 42, No. 6, June 2004

Evolution of Localized Vortex Disturbance in Uniform Shear Flow: Numerical Investigation

Victoria Suponitsky,* Jacob Cohen,† and Pinhas Z. Bar-Yoseph‡
Technion—Israel Institute of Technology, 32000 Haifa, Israel

The possibility that a simple model of interaction between a localized vortical disturbance and laminar uniform unbounded shear flow is capable of reproducing the generation mechanism and characteristics of coherent structures naturally occurring in wall bounded turbulent flows is examined numerically. Gaussian and toroidal vortices are used as the initial disturbances. The concentrated vorticity field of the Gaussian vortex is defined by a single length scale δ, which is assumed to be much smaller than the characteristic scale of the base flow. The toroidal disturbance is defined by two length scales r_0 and δ, corresponding to the radius and thickness of the torus, respectively. For a small-amplitude Gaussian disturbance, the numerical solution of the full Navier–Stokes equations agrees well with the analytical solution of the linearized vorticity equation. Accordingly, the disturbance, independent of its initial geometry, eventually evolves into a pair of counter-rotating quasi-streamwise vortices and an associated low-speed streak. Moreover, an optimal range of r_0/δ is found for which the spanwise separation of the two elongated vortical regions, expressed in wall units, corresponds well to the spacing of streaks and hairpin vortex legs observed in turbulent flows. Preliminary results show that a large-amplitude disturbance, independent of its initial geometrical shape, eventually evolves into a hairpin vortex.

Introduction

WALL-BOUNDED turbulent shear flows are characterized by unsteady, seemingly chaotic motion. In fact, however, the motion is not random, and it has been observed to be governed by well-organized vortical structures. These turbulent shear flows are known to consist mainly of two different kinds of coherent vortical structures: counter-rotating streamwise vortices, which lead to the formation of low- and high-speed velocity regions (streaks), observed in the near-wall region and hairpin-shaped vortices extended across the boundary layer. The two kinds of coherent structures were experimentally first identified by Kline et al.[1] in 1967. The main experimental and numerical findings regarding the coherent structures are discussed and summarized by Robinson,[2] by Smith and Walker,[3] and more recently by Schoppa and Hussain.[4]

One of the remarkable features of these coherent structures is that their characteristic length scales (expressed in wall units) remain almost unchangeable for various kinds of shear flows and over a significant range of Reynolds numbers. Moreover, their evolutionary dynamics, as well as characteristic length scales, have been found to be similar in both fully turbulent and transitional shear flows. Therefore, to understand the underlying physics of the coherent structures in turbulent flows, several authors have studied the evolution of similar structures artificially generated in subcritical wall-bounded laminar shear flows, instead of a fully turbulent environment. The advantages of this approach are that the flow is quiet, and therefore, it is easy to identify and follow the evolution of the vortical structure and to control and examine the parameters of the flow associated with the coherent structure. The disadvantage of this approach is that the influence of the turbulent Reynolds stress associated with other vortical structures is ignored.

Received 16 June 2003; presented as Paper 2003-3603 at the AIAA 33rd Fluid Dynamics Conference, Orlando, FL, 23–26 June 2003; revision received 8 December 2003; accepted for publication 4 February 2004.

*Graduate Student, Faculty of Aerospace Engineering. Student Member AIAA.
†Associate Professor, Faculty of Aerospace Engineering.
‡Professor, Faculty of Mechanical Engineering.

Blackwelder[5] compared the constituent elements of the counter-rotating streamwise vortices for both transitional and turbulent boundary layers and suggested that the dynamics of the vortices are similar. The evolution of a localized disturbance in a laminar shear flow was studied numerically and experimentally by Breuer and Haritonidis[6] and Breuer and Landahl.[7] They reported that the elongated low- and high-speed regions that develop as the disturbance progresses are reminiscent of high- and low-speed streaks that are observed in fully turbulent wall flows. Similar observations were reported by Henningson et al.,[8] who investigated the evolution of a localized disturbance in laminar plane Poiseuille flow.

Hairpin vortices (or horseshoe vortices) were artificially generated in a laminar boundary layer, for example, by Acarlar and Smith,[9] in a rotating axisymmetric laminar Couette flow by Malkiel et al.,[10] and more recently in laminar air channel flow by Svizher and Cohen.[11]

Levinski and Cohen[12] proposed a general model characterizing the evolution of three-dimensional localized disturbances, the dimensions of which are smaller than characteristic length scale of the external shear flow. According to their model, a simple feedback mechanism takes place: The lift up of the disturbance in the vertical direction stretches the external spanwise vorticity field and generates a disturbed vorticity component in the vertical direction. The direct effect of the external shear flow is to rotate the disturbed vortex back toward the wall and thereby to amplify the streamwise vorticity component. The new streamwise vorticity component induces an additional vertical velocity, which further enhances the lift-up effect and closes the feedback loop.

Note that according to the linear stability theory the uniform shear flow is predicted to be stable with respect to exponentially growing (normal modes) three-dimensional infinitesimally small disturbances. However, disturbances having a spanwise structure may experience an algebraic (transient for the viscous flow) growth mechanism. The latter growth mechanism was first demonstrated by Ellingsen and Palm[13] for streamwise independent disturbances in 1975. Later, this mechanism was extensively studied by many investigators.[8,14–19]

The similarity of developed vortical structures occurring in completely different fully developed bounded turbulent flows as well as in transitional flows suggests the existence of a basic mechanism responsible for the formation of these vortical structures, under various base flow conditions. The common elements for all flows are the shear of the base flow and the presence of some kind of a vortical disturbance having a spanwise structure. The purpose of the

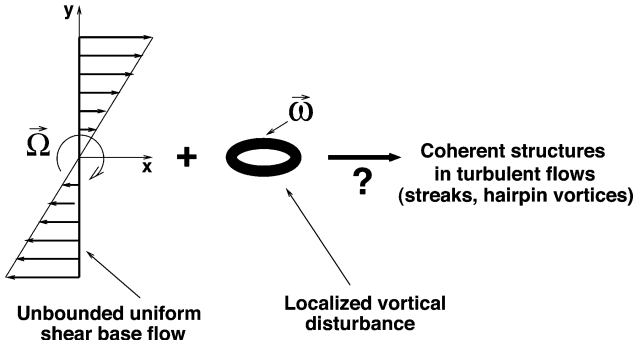

Fig. 1 Schematic of the research objective.

present research is to examine numerically the possibility that a simple model of interaction between a localized vortical disturbance and laminar uniform unbounded shear flow is capable of reproducing the generation mechanism and characteristics of coherent structures naturally occurring in turbulent boundary flows. This objective is shown schematically in Fig. 1. The unbounded uniform shear base flow is characterized by its shear $\boldsymbol{\Omega} = (0, 0, \Omega_z)$, whereas the localized disturbance is characterized by its vorticity field $\boldsymbol{\omega}$. The disturbance amplitude is defined as the ratio between the disturbance maximum vorticity magnitude $\omega_{\max}$ and the shear of the base flow. When the disturbance amplitude is much smaller than 1, the disturbance is considered to be a small-amplitude disturbance, and its evolution is governed by the linearized equations. The role of the wall in this model is only to maintain a shear base flow and to generate the initial disturbance, the dimensions of which are much smaller than a typical scale representing the velocity gradient of the external flow, whereas its effect on the disturbance evolution is sought to be negligible.[12]

Unlike some previous works where the term localized disturbance referred to disturbances having their smallest typical length scale of the order of the boundary-layer thickness, for example, Refs. 6–8 and 20, in the present investigation all of the disturbance dimensions are much smaller than the characteristic length scale of the base flow.

In this paper, we mainly focus on the evolution of small-amplitude disturbances and, in particular, on the effects of the initial disturbance geometry and Reynolds number. Although some preliminary results of the nonlinear case are included for the sake of completeness, the detailed investigation of the nonlinear effect is beyond the scope of the present paper but that study will be published in the near future.

The temporal evolution of localized vortical disturbances of different geometrical shapes and Reynolds numbers is obtained by the solution of the full Navier–Stokes equations. For the particular case in which an initial small-amplitude disturbance has a spherical Gaussian vorticity distribution, the numerical results are validated by the comparison with the corresponding analytical solution for a small-amplitude disturbance, recently obtained by Shukhman and Levinski.[21]

In the next section the initial disturbance is described, and the governing parameters of the problem are defined. Then the numerical procedure is detailed, and a comparison with the analytical solution for an initial Gaussian vortex disturbance is carried out. The effects of the initial disturbance geometry and the Reynolds number are then discussed, and finally the main results are summarized and discussed.

Problem Statement

The purpose of the present work is to study the evolution of a localized (in all three dimensions) vortical disturbance embedded in uniform shear flow. Here we shall mainly focus on small-amplitude perturbations. In the following sections, the initial disturbance shapes, governing parameters, and evolutionary characteristics are described.

Initial Disturbance

In general, any vortex that is localized in space (in all three dimensions) with a divergent free vorticity field can be used as an initial disturbance. In the present work, two different shapes of the initial localized vortical disturbance are studied. The first one is a spherical vortex ring with Gaussian vorticity distribution, which is defined as

$$\boldsymbol{\omega} = -\boldsymbol{p} \times \nabla F, \qquad F = \left(\pi^{\frac{1}{2}}\delta\right)^{-3} \exp\left(-r_s^2 \big/ \delta^2\right) \tag{1}$$

where $\boldsymbol{\omega}$ is the vorticity vector, $\boldsymbol{p}$ is a vector defining its space orientation, r_s is a spherical radial coordinate, and δ is a representative length scale of the disturbance. (If the function F [Eq. (1)] is normalized such that

$$\int_V F \, \mathrm{d}V = 1$$

then the vector $\boldsymbol{p}$ is the fluid impulse of the initial vortical disturbance.) The disturbance maximum vorticity is obtained at $r_s = \delta/\sqrt{2}$. This disturbance, having a single length scale, serves as an example of a localized (in all three dimensions) region of concentrated vorticity, with vorticity lines forming circles in a plane perpendicular to the direction of the vector $\boldsymbol{p}$. An example of the Gaussian disturbance, initially having horizontal orientation, shown by the isosurfaces of the vorticity magnitude, is presented in Fig. 2 for the two different threshold levels of the vorticity magnitude. The associated vorticity vectors are also shown to clarify the structure of the vorticity field. The amplitude of the disturbance and its initial orientation are defined by magnitude and direction of the vector $\boldsymbol{p}$, respectively, and the size of the localized vorticity region is defined by the length scale δ.

The second shape of the initial vortex disturbance, considered in the present investigation, is a horizontal (xz plane) torus having the following vorticity field:

$$\boldsymbol{\omega} = \begin{Bmatrix} z \\ 0 \\ -x \end{Bmatrix} A \exp\left(\frac{-y^2}{\delta^2}\right) \exp\left[\frac{-(r - r_0)^2}{\delta^2}\right] \tag{2}$$

where x, y, and z are the streamwise, normal, and spanwise directions, respectively, A is a positive constant defining the strength of the disturbance, $r = \sqrt{(x^2 + z^2)}$ is a radial cylindrical coordinate, and r_0 and δ are two characteristic length scales. This initial disturbance has a vorticity distribution similar to that of the Gaussian vortex. (For the horizontal torus the vorticity lines form circles in the xz plane.) However, the existence of the two characteristic length scales allows us to vary the localized properties of the disturbance and seek the optimal aspect ratio for which the disturbance growth is maximal. Note that any orientation other than the horizontal one

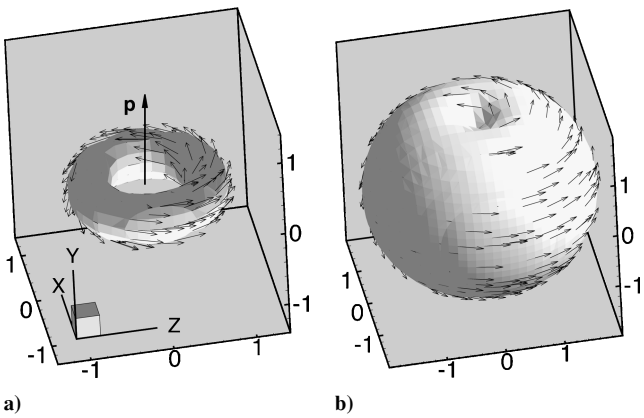

Fig. 2 Isosurfaces of the vorticity magnitude and the associated vorticity vectors of an initial horizontal Gaussian disturbance: a) $\|\omega\|/\omega_{\max} = 0.9$ and b) $\|\omega\|/\omega_{\max} = 0.1$.

of the toroidal disturbance relative to the base flow can be achieved by a suitable rotation of the coordinate system. An example of the toroidal disturbance, initially with horizontal orientation, shown by the isosurfaces of the vorticity magnitude is presented in Fig. 3 for the two different threshold levels of the vorticity magnitude. The associated vorticity vectors are also shown to clarify the structure of the vorticity field. From Eq. (1), it can be seen that the vorticity magnitude for the Gaussian vortex is proportional to

$$\|\boldsymbol{\omega}\| \sim r_s \cdot \exp\left(-r_s^2 \big/ \delta^2\right) \tag{3}$$

whereas for the toroidal disturbance is given by

$$\|\boldsymbol{\omega}\| \sim r \cdot \exp(-y^2/\delta^2) \exp\left(-(r - r_0)^2 \big/ \delta^2\right) \tag{4}$$

When $r_0 = 0$ is substituted into Eq. (4), the distribution of the vorticity magnitude is reduced to that of the Gaussian vortex (3), except that r_s and r in both expressions refer to the spherical and radial coordinates, respectively. Thus, the Gaussian disturbance can be considered as an approximate limit of the toroidal disturbance.

To demonstrate the role of the two characteristic length scales, normalized distributions (each by its own maximum) of the vorticity magnitude along the x axis for the Gaussian and the toroidal disturbances with several r_0/δ ratios are plotted in Fig. 4. From Fig. 4, one can deduce that r_0 and δ are associated with the radius of the torus and the thickness of the concentrated vorticity region, respectively.

Governing Parameters

Once the shape of the initial vortical disturbance is chosen, there are three parameters that govern the flow. The first one is the strength of the initial disturbance ε, which is defined by the amplitude ratio between the maximum vorticity of the disturbance, $\omega_{\max}$, and the shear of the base flow, Ω, that is,

$$\varepsilon = \omega_{\max} / \Omega \tag{5}$$

The second governing parameter is the orientation of the initial disturbance relative to the direction of the base flow, which is given in terms of the angle ϕ between the direction normal to the plane of the torus (the direction of the vector $\boldsymbol{p}$) and the positive direction of the x axis (Fig. 5). The third governing parameter is the Reynolds number (see Ref. 21), which is based on the characteristic length scale δ,

$$Re = \Omega\delta^2/\nu \tag{6}$$

We shall use δ and $1/\Omega$ as reference lengthscale and timescale, respectively, to normalize all dimensional variables. Accordingly, $X = x/\delta$, $Y = y/\delta$, $Z = z/\delta$, and $T = t\Omega$.

The effect of the initial amplitude and orientation, with regard to a Gaussian vortex, were studied by Suponitsky et al. in Refs. 22 and 23, respectively. (Data also available at http://tx.technion.ac.il/~/cml/cml/staff/vika.htm [cited 23 May 2003].) The effects of the Reynolds number and the geometrical shape of the initial disturbance are the main subjects of the present paper.

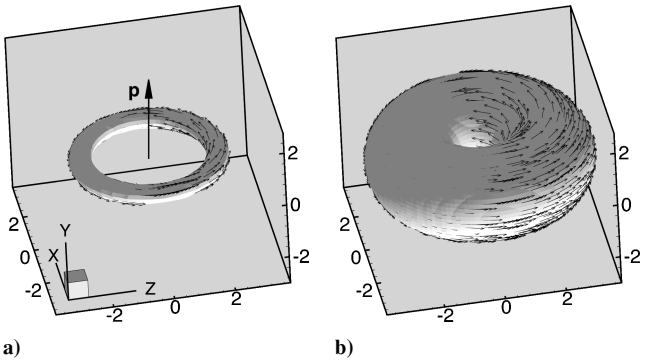

Fig. 3 Isosurfaces of the vorticity magnitude and the associated vorticity vectors of an initial horizontal toroidal disturbance ($r_0/\delta = 2$): a) $\|\omega\|/\omega_{\max} = 0.9$ and b) $\|\omega\|/\omega_{\max} = 0.1$.

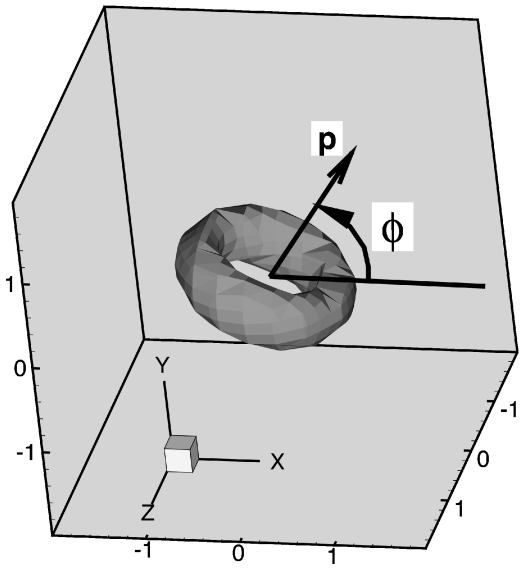

Fig. 5 Definition of ϕ: the angle between the direction of the vector p and the positive direction of the x axis.

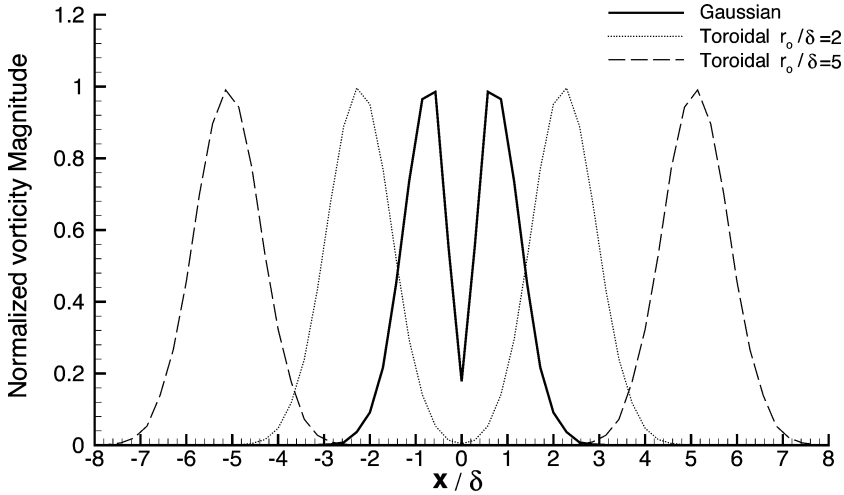

Fig. 4 Normalized vorticity magnitude distribution along the x axis for different geometrical shapes.

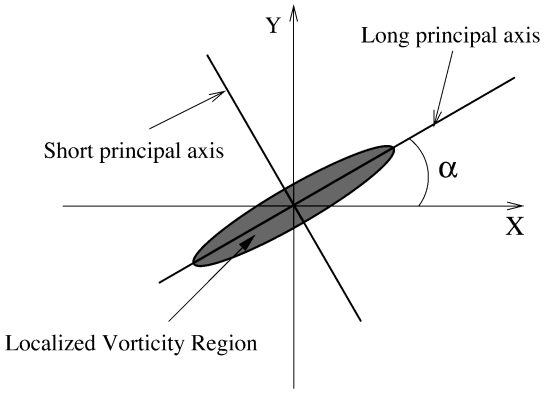

Fig. 6 Schematic of the principal axes calculated from TED.

Vortex Characteristics

In the present work, the vortical structure is identified by the isosurfaces of the vorticity magnitude. The inclination angle α of the vortical structure with respect to the positive direction of the x axis is defined with the aid of the tensor of enstrophy distribution (TED).[21] The definition of TED is given by

$$T_{ij}(t) = \int_V \|\boldsymbol{\omega}(t)\|^2 x_i x_j \, \mathrm{d}V \tag{7}$$

The angle α is defined as the angle between the long principal axis calculated from TED and the positive direction of the x axis (Fig. 6). Its expression for the case in which $p_z = 0$ is given by[21]

$$\alpha = \frac{1}{2}\arctan\left(\frac{2T_{12}}{T_{11}-T_{22}}\right) + \frac{\pi}{4}(1+s) - \frac{\pi}{2}$$
$$s = \mathrm{sign}(T_{11}-T_{22}) \tag{8}$$

The strength of the vortical disturbance W is measured by integrating the enstrophy over the entire volume, that is,

$$W(t) = \int_V \|\boldsymbol{\omega}(t)\|^2 \, \mathrm{d}V \tag{9}$$

Numerical Procedure

Full unsteady incompressible Navier–Stokes equations for primitive variables (velocity components and pressure) are solved by the finite volume method using the commercial computational fluid dynamics (CFD) code FLUENT.[24]

The schematic of the computational domain and the coordinate system definition is shown in Fig. 7. The goal is to simulate numerically the evolution of a localized vortical disturbance in an unbounded uniform shear flow. For most of the computations, the size of the computational domain is $80\delta \times 30\delta \times 50\delta$ along the streamwise x, walls-normal y, and spanwise z directions, respectively, and the whole computational domain has about 1.3 million grid nodes. For the Gaussian case, a domain size of $40\delta \times 40\delta \times 30\delta$ with about one million grid nodes was found to be sufficient. For all simulations, this size of the computational domain is sufficiently large (relative to the size of the initial disturbance) so that the effect of the finite computational domain on the disturbance development is negligible.

The initial vortical disturbance is placed at the center of the computational domain. The uniform shear base flow velocity profile is obtained numerically as a steady solution of the laminar two-dimensional Couette flow with zero pressure gradient. Accordingly, the moving walls boundary conditions are $u(y = 20\delta) = U_0$ and $u(y = -20\delta) = -U_0$. Along the streamwise direction x and spanwise direction z the periodic and the symmetry boundary conditions

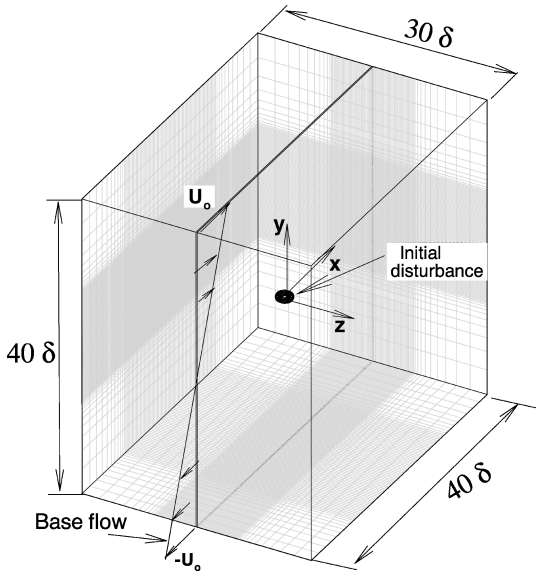

Fig. 7 Schematic of the computational domain: x streamwise direction, y transverse direction, and z spanwise direction.

are employed, respectively. For each simulation, the initial disturbance is superimposed on the base flow. Because the initial disturbance is given in terms of a vorticity field, the corresponding velocity distribution must first be calculated to provide the initial velocity field needed for the CFD code. For the particular case in which the disturbance is described by the function $F = F(r_s)$ [Eq. (1)], an analytical velocity distribution exists[21]:

$$u_i = F(r_s)\left[p_i - x_i(\boldsymbol{p}\cdot\boldsymbol{r}_s)/r_s^2\right] - \left[H(r_s)/r_s^3\right]\left[p_i - 3x_i(\boldsymbol{p}\cdot\boldsymbol{r}_s)/r_s^2\right] \tag{10}$$

where

$$H(r_s) = \int_0^{r_s} F(\xi)\xi^2 \, \mathrm{d}\xi, \qquad u_i(0) = \frac{2}{3}p_i$$

For any other localized vorticity distribution, the corresponding velocity field for incompressible flow is given by[25]

$$\boldsymbol{u}(x,y,z) = -\frac{1}{4\pi}\int_V \frac{\boldsymbol{s}\times\boldsymbol{\omega}'}{s^3}\,\mathrm{d}V' \tag{11}$$

where

$$\boldsymbol{s} = (x-x', y-y', z-z')$$
$$s = \|\boldsymbol{s}\| = \sqrt{(x-x')^2 + (y-y')^2 + (z-z')^2}$$

For most of the simulations, the size of the initial vortical disturbance and the shear of the base flow are $\delta = 1$ mm and $\Omega = 40$ 1/s, respectively. These parameters are chosen in accordance with the experiments carried out with a Taylor–Couette apparatus (see Ref. 10). For this set of parameters, the relevant Reynolds number is $Re = \Omega\delta^2/\nu = 40$. Nevertheless, for $\Omega = 40$ 1/s, the Reynolds number, based on the absolute velocity of the moving walls and the distance between them, is 3.2×10^4. This Reynolds number is close to the upper limit for obtaining numerically the known laminar steady plane–Couette solution.

Results

Comparison Between Analytical and Numerical Solutions

In this section, we present the comparison between the analytical viscous and inviscid solutions of the three-dimensional linearized vorticity equation[21] and the numerical solution of the full Navier–Stokes equations for the case of a small-amplitude ($\varepsilon \ll 1$) Gaussian

initial disturbance with a horizontal orientation. Two disturbances are considered to have $\varepsilon = 0.015$ and $\varepsilon = 0.375$ initial amplitudes. The comparison is carried out for $Re = 40$. To examine the effect of viscosity, the inviscid analytical solution[21] is also included.

The distributions of the vorticity magnitude along the x and z axes are shown in Fig. 8. The results obtained from the numerical solution are normalized to match the analytical solution identically at $T = 0$. Also note that at $T = 0$ the streamwise and spanwise distributions are identical. It is evident that the numerical solutions follow closely the viscous analytical ones for both amplitudes ($\varepsilon = 0.015$ and 0.375) of the initial disturbances during the entire evolution. Because of the symmetrical properties of the initial disturbance, for example, $p_z = 0$, the distribution of the vorticity magnitude along the z axis (Fig. 8b) remains symmetric around $Z = 0$ during the entire evolution. On the other hand, the symmetrical distribution of the vorticity magnitude along the x axis (Fig. 8a) is due to the symmetrical properties of the linearized equations. Once the disturbance is sufficiently large, this symmetry is broken by nonlinear effects (Fig. 8a) at $T \geq 2$ for the disturbance with an initial amplitude of $\varepsilon = 0.375$). Comparing the inviscid and viscous solutions, one can see that the shape of the vorticity magnitude distribution is well preserved by the inviscid solution, whereas its actual magnitude is severely overestimated. Finally, note that the vorticity magnitude along x axis is significantly decreased during the first stages of evolution (up to $T = 2$) and then increases again at longer times. This is attributed to the generation of spanwise vorticity sheets during the disturbance evolution process, which will be discussed in the following sections.

Effect of the Initial Disturbance Shape

In this section, the geometrical shape, the inclination angle, and the strength of the vortical structures associated with a Gaussian

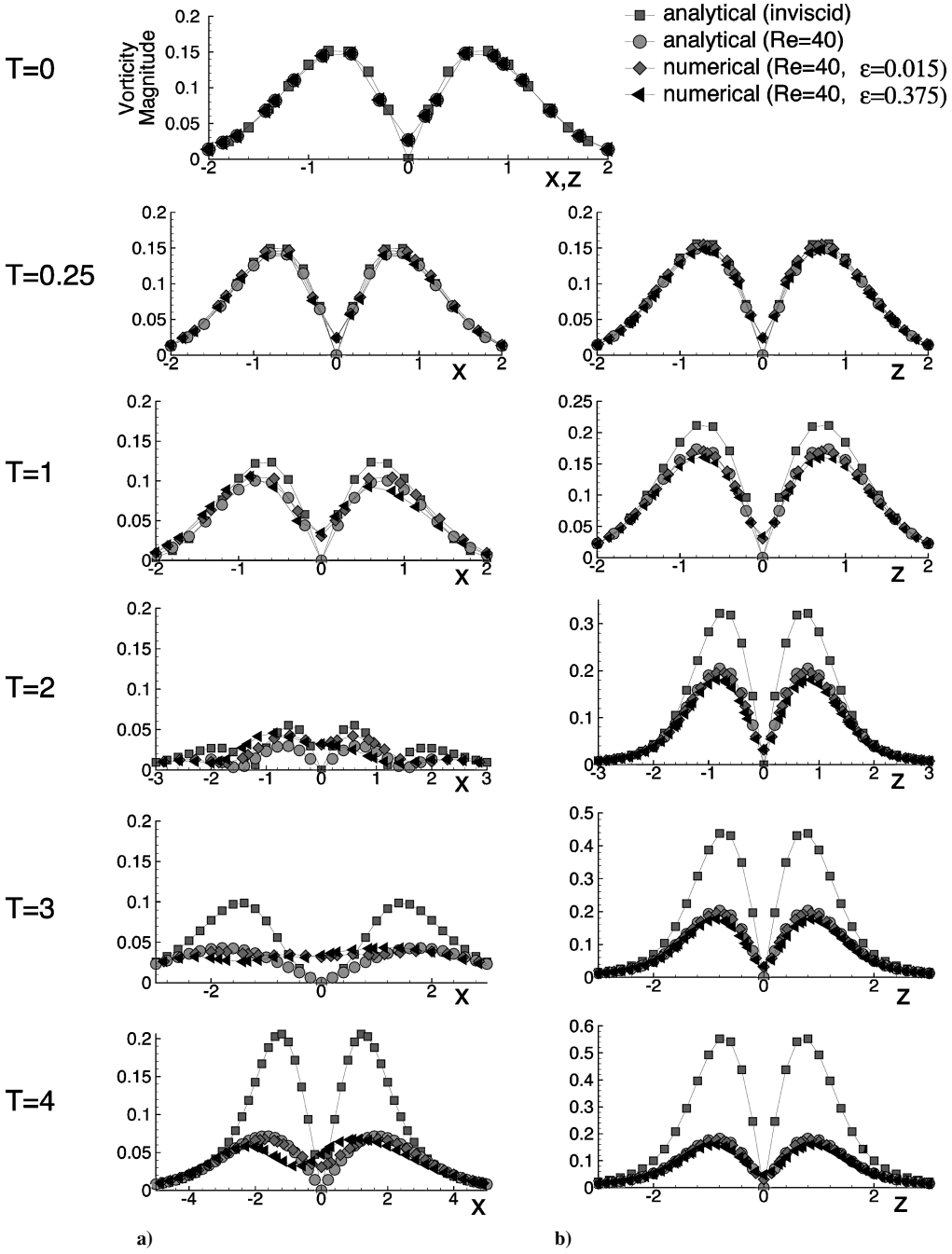

Fig. 8 Comparison between analytical and numerical results for temporal evolution of the vorticity magnitude distribution of an initially horizontal Gaussian disturbance: a) distribution along x axis and b) distribution along z axis.

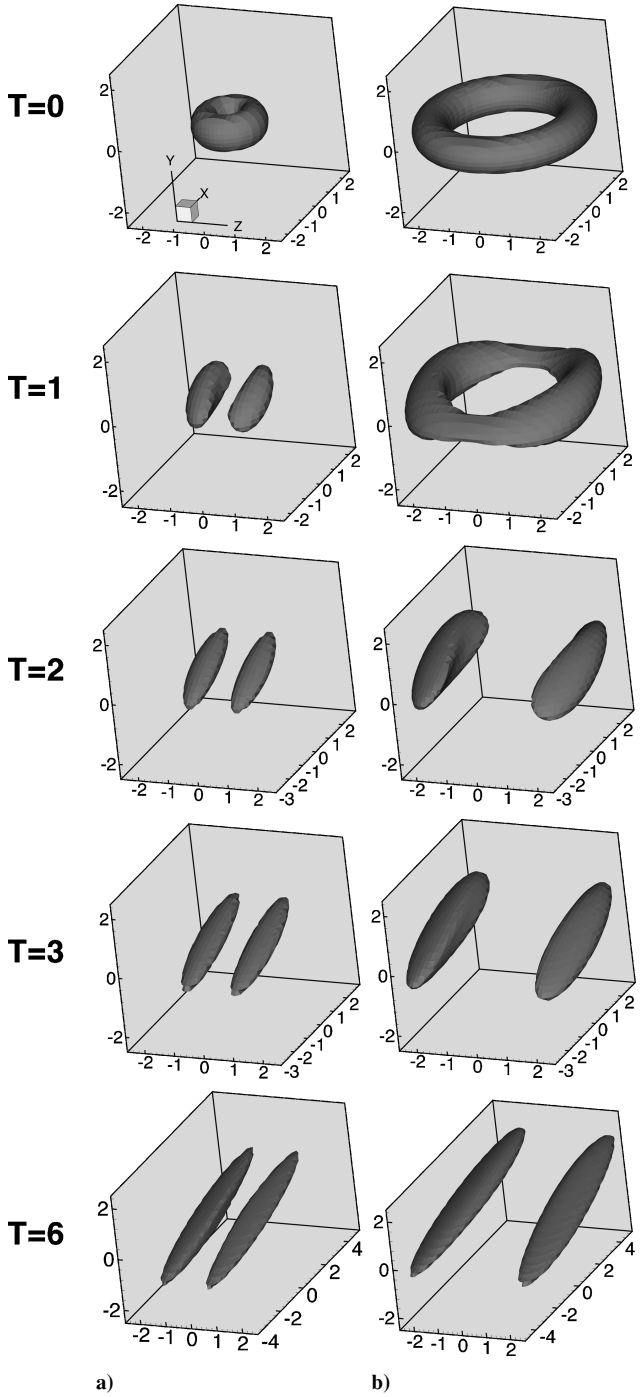

Fig. 9 Evolution of small amplitude ($\varepsilon = 0.375$) disturbances shown by isosurfaces of the vorticity magnitude ($\|\omega\|/\omega_{\max} = 0.7$): a) Gaussian disturbance and b) toroidal disturbance ($r_0/\delta = 2$).

and various toroidal initial disturbances are studied and compared during their temporal evolution. All other parameters are held constant, namely, the initial amplitude and orientation are $\varepsilon = 0.375$ and $\phi = 90$ deg, respectively, and the Reynolds number, based on δ, is $Re = 40$. Thus, the effect of the length scales ratio (r_0/δ) can be explored.

The temporal evolutions of a small-amplitude Gaussian and toroidal ($r_0/\delta = 2$) disturbances are shown in Fig. 9 using isosurfaces of the vorticity magnitude with a threshold level of $\|\omega\|/\omega_{\max} = 0.7$. The projections of these isosurfaces on the xy plane are shown in Fig. 10. Also shown in Fig. 10 is the long principal axis calculated from TED and indicated by the black solid line. The resulted vortical structure extracted by the vorticity magnitude isosurface for $\|\omega\|/\omega_{\max} = 0.6$, and the streamwise u and vertical v velocity components distributions along the long principal axis at $Z = 0$ are

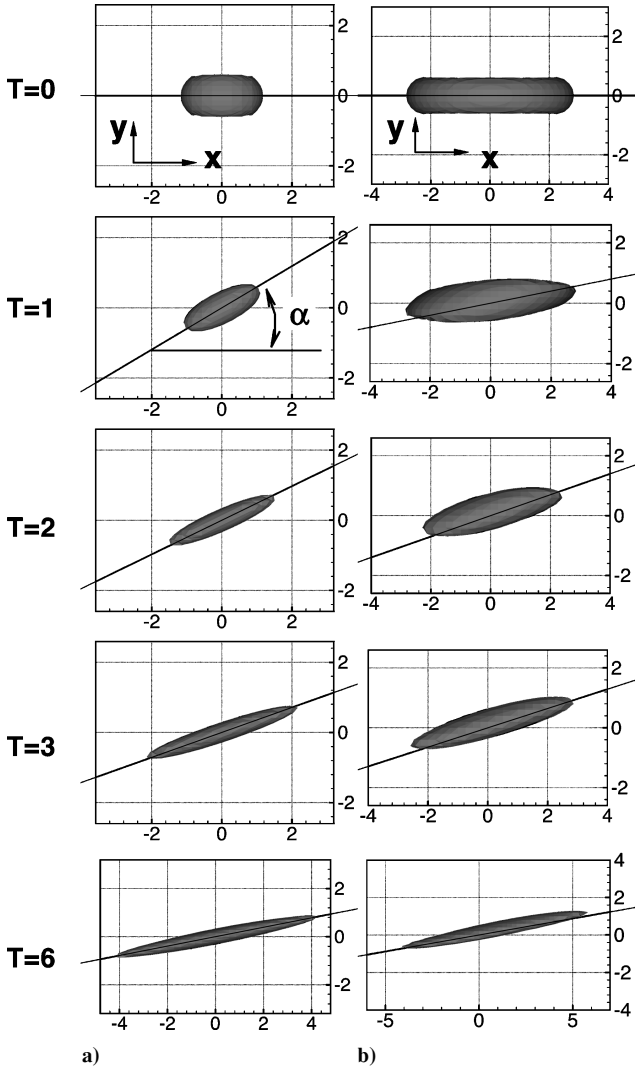

Fig. 10 Vorticity magnitude isosurfaces ($\|\omega\|/\omega_{\max} = 0.7$) projected on the xy plane; a) Gaussian disturbance and b) toroidal disturbance ($r_0/\delta = 2$): ——, long principal axis (calculated from TED).

shown in Figs. 11a and 11b, respectively, for the Gaussian vortex disturbance at $T = 6$.

Figure 9 shows that both disturbances quickly evolve into pairs of quasi-streamwise counter-rotating elongated vortices, similar to the ones observed in the near-wall region of a turbulent boundary layer. From the projection of the isosurfaces on the xy plane (Fig. 10), we can see that both disturbances, initially with horizontal orientation, rotate around the z axis, but their rotation rate as well as their inclination angle α (between the long principal axis and positive direction of the x axis) are different. It is also evident that the visual inclination angle of the vortical structure corresponds well to the angle α calculated from TED for both initial disturbance geometries during the whole evolution.

During the disturbance evolution, spanwise vorticity sheets ω_z, which bridge the pair of quasi-streamwise counter-rotating elongated vortices, are generated and can be seen when isosurfaces of a lower threshold level of the vorticity magnitude are drawn (Fig. 11a). The formation of these vorticity sheets and their subsequent strengthening can explain the increase of the vorticity magnitude along the x axis at relatively long times mentioned in the preceding section (Fig. 8a) for $T = 3$ and 4. To explain the generation of the spanwise vorticity sheets, note (Introduction section) that the disturbance evolution is governed by a transient growth mechanism. Accordingly, the negative streamwise velocity component increases, while the vertical one decays (Fig. 11b). Thus, at long times local shear layers between the induced negative streamwise velocity and the base flow are formed. The spanwise vorticity sheets

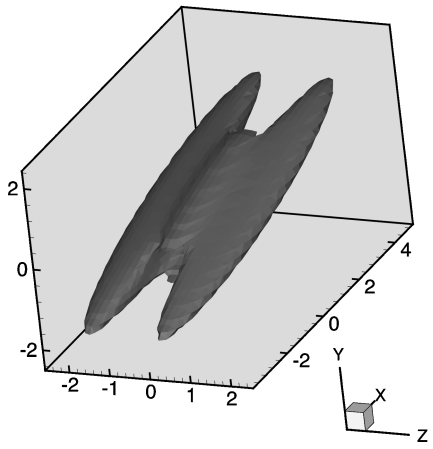

Fig. 11a Vorticity magnitude isosurface ($\|\omega\|/\omega_{max} = 0.6$).

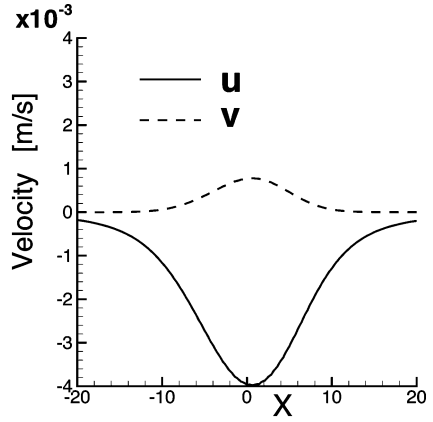

Fig. 11b Velocity components u and v distributions along the long principal axis of the vortex at $Z = 0$; Gaussian vortex initial disturbance $T = 6$.

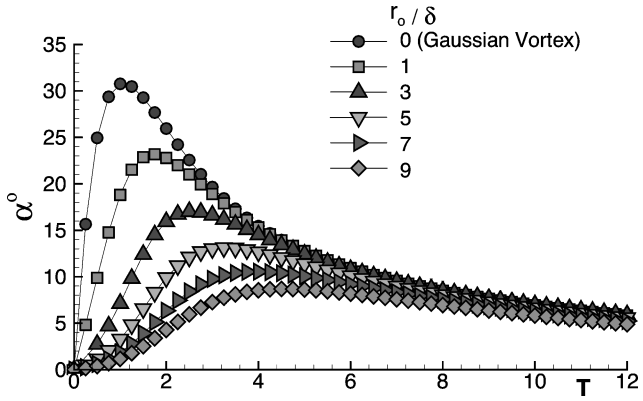

Fig. 12 Temporal evolution of the vortical structure inclination angle α.

shown in Fig. 11a are the evidence of these local vertical shear layers. (For more details, see Suponitsky et al.[22])

The effect of the initial disturbance geometry, expressed by the length scales ratio r_0/δ, on the temporal evolution of the vortical structure inclination angle α is shown in Fig. 12. The angle α is calculated from TED and is found to correlate well with the visual inclination angle for the different initial disturbance geometries. Figure 12 shows that all disturbances, initially horizontal, rotate around the z axis during the first stages of evolution. Then, after reaching a maximum angle, the vortical structures rotate in the opposite direction, and eventually the angles of all collapse on a single slowly decreases curve independent of their initial geometrical shapes. Note that the angles at longer times ($T > 10$) are less than 10 deg. The rate of rotation and the maximum inclination angle are functions of the initial disturbance geometry. The maximum angle of rotation (about 30 deg) is attained by the Gaussian vortex at the shortest time ($T = 1$). When the ratio r_0/δ is increased, the time at which the maximum inclination angle is attained is increased, whereas the value of the angle itself is decreased. For an initial toroidal disturbance with $r_0/\delta = 9$, the maximum angle is about 9 deg attained at $T \approx 4$.

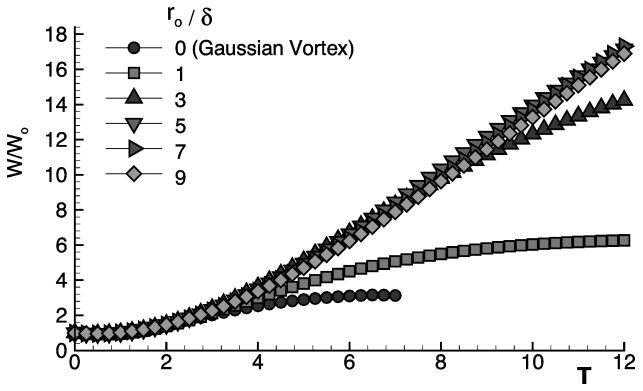

Fig. 13 Temporal evolution of the normalized enstrophy integral W/W_0.

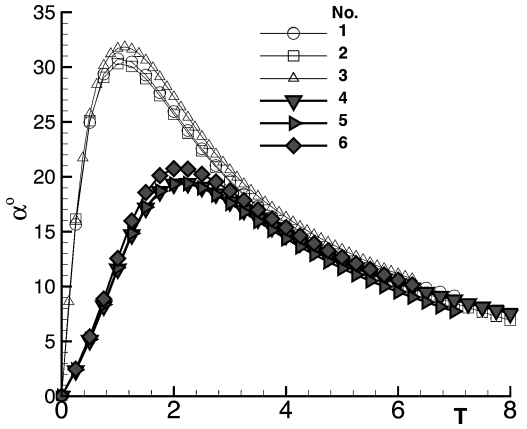

Fig. 14 Temporal evolution of the vortical structure inclination angle α.

The temporal evolution of the normalized enstrophy integral $[W/W_0$, where $W_0 = W(T = 0)]$ is shown in Fig. 13. It can be seen that the disturbance initial geometrical shape plays a very important role on its transient growth. The Gaussian vortex attains the weakest growth, the maximum of which is less than 3.8 by $T \approx 6$. Then the strength of this vortex decays due to viscous effects. Increasing the ratio r_0/δ results in a more significant transient growth, which is attained at longer times. For the disturbance with $r_0/\delta = 5 \div 7$, the initial enstrophy integral is amplified by a factor of 18 by $T = 12$, and it still continues to grow. However, further increasing the length scales ratio r_0/δ results in the reduction of the transient growth. Thus, the initial disturbances with length scales ratio within the range of $r_0/\delta = 5 \div 7$ are optimal, that is, they lead to the maximum transient growth.

Note, as it can be seen from Fig. 9, that the spanwise separation distance between the two elongated vortical regions remains approximately constant during the disturbance evolution and can be approximated as $2r_0$. This distance, expressed in terms of wall units $[y^+ = yu^*/\nu;\ u^* = \sqrt{(\tau_w/\rho)}]$ lies within the range of $63 < y^+ < 113$ for the disturbances with length scale ratio r_0/δ between $5 < r_0/\delta < 9$. In this respect, note that the spanwise spacing between low-speed streaks in turbulent boundary layers is about 100 wall units. In addition, the spanwise separation of hairpin legs in fully developed turbulent shear flows is usually about 50–60 wall units and does not exceed 100.

This suggests that the spanwise separation distance between the streaks or hairpin legs observed in wall-bounded shear flows is

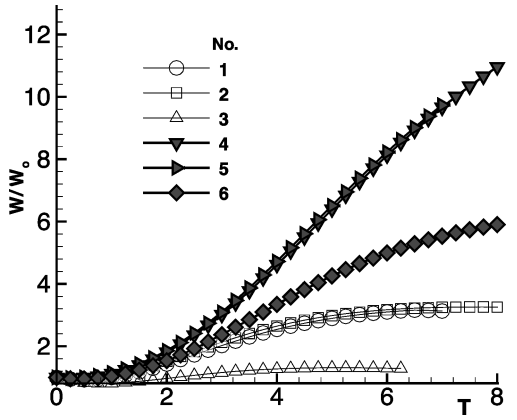

Fig. 15 Temporal evolution of the normalized enstrophy integral W/W_0.

probably due to their optimal transient growth, similar to the one observed in our simple model.

Effect of Disturbance Reynolds Number

The results for a fixed Reynolds number ($Re = 40$), where the Reynolds number is based on δ [Eq. (6)], were presented in the preceding section. The length scale δ was also used to define the Reynolds number for the toroidal disturbance. Note that the toroidal disturbance is defined by two length scales [Eq. (4)]. Therefore, two nondimensional parameters are required to described its evolution, that is, $Re = \Omega\delta^2/\nu$ and r_0/δ. In the sequel, the evolution of an initial disturbance with various combinations of these parameters is considered. The flow parameters for these simulations are given in Table 1, for the Gaussian (G) and toroidal (T) disturbances, respectively. The initial amplitude is $\varepsilon = 0.375$, the initial orientation is $\phi = 90$ deg, and $\nu = 1 \times 10^{-6}$ m^2/s for all simulations. Note that for a given set of nondimensional parameters, two different combinations of the corresponding dimensional parameters are used.

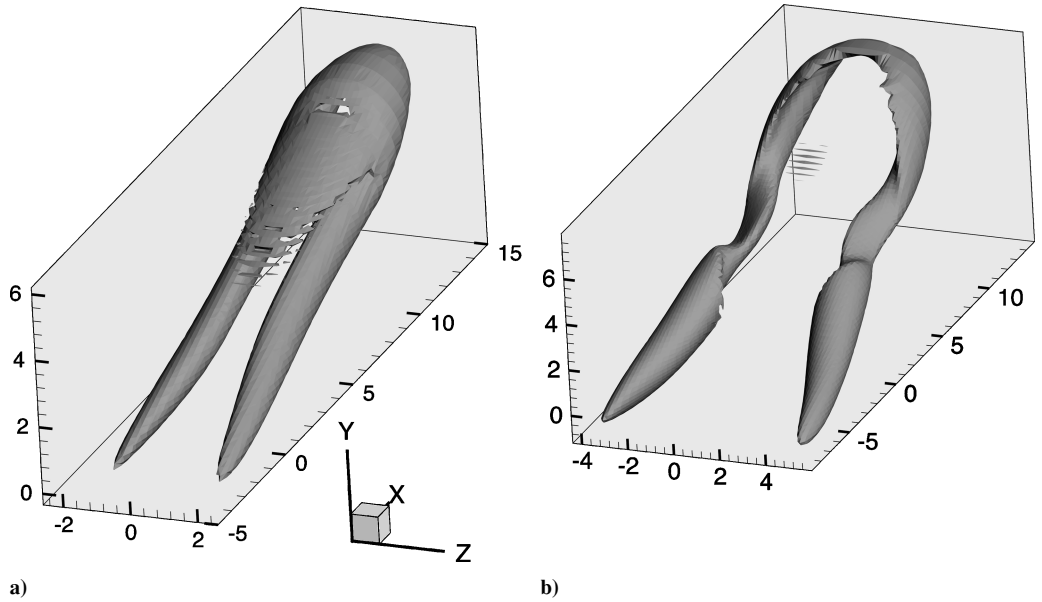

Fig. 16 Hairpin vortex developed from large-amplitude disturbance and shown by isosurfaces of the vorticity magnitude, $\|\omega\|/\omega_{\max} = 0.5$, $Re = 40$, and $T = 5$): a) Gaussian disturbance, $\varepsilon = 7.5$ and b) toroidal disturbance ($r_0/\delta = 3$), $\varepsilon = 5$.

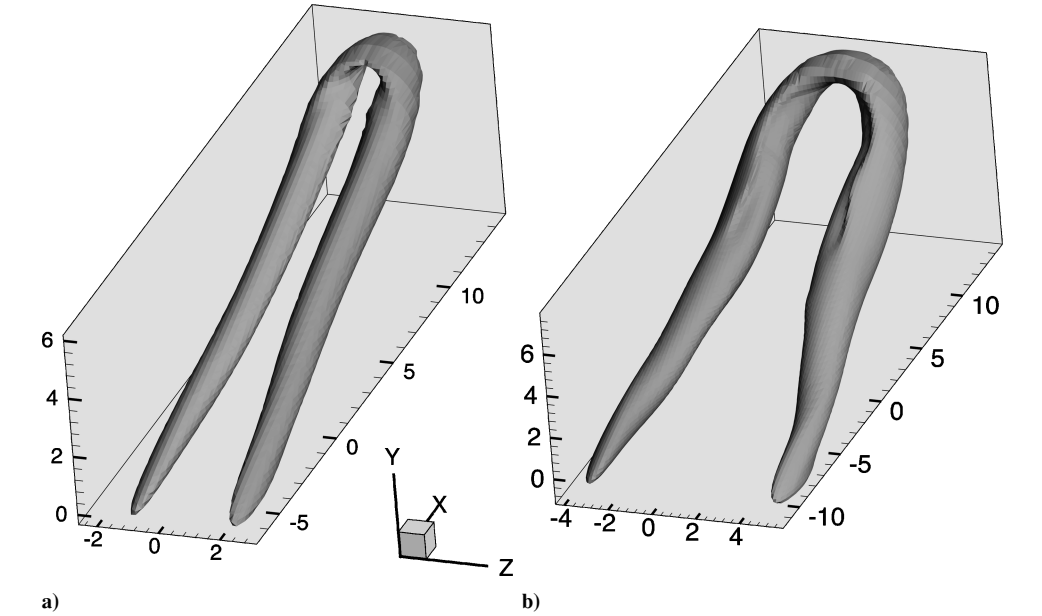

Fig. 17 Hairpin vortex developed from large-amplitude disturbance and shown by isosurfaces of the positive second invariant Q of the velocity gradient tensor, $Q/Q_{\max} = 0.05$, $Re = 40$, and $T = 5$: a) Gaussian disturbance, $\varepsilon = 7.5$ and b) toroidal disturbance ($r_0/\delta = 3$), $\varepsilon = 5$.

Table 1 Flow parameters for the simulations

Number	Geometry	Re	δ, mm	r_0/δ	Ω, 1/s
1	G	40	1	——	40
2	G	40	$\sqrt{2}$	——	20
3	G	20	1	——	20
4	T	40	1	2	40
5	T	40	$\sqrt{2}$	2	20
6	T	20	1	2	20

In Figs. 14 and 15, the temporal evolutions of α and W/W_0 are presented for the cases given in Table 1. Figure 14 shows that the kinematics of the disturbance evolution depends only on its initial shape, determined by the ratio (r_0/δ). The strength of the vortex, on the other hand, strongly depends on the Reynolds number (Fig. 15). As the Reynolds number is increased for a given geometry, the transient growth of the disturbance increases as well. The normalized time $T = t \cdot \Omega$, by which the enstrophy integral reaches its maximum value before starting to decay due to the viscous effects, increases with the Reynolds number.

Nonlinear Initial Disturbance

The vortical structures resulted from an initially horizontal Gaussian and a toroidal $(r_0/\delta = 3)$ disturbances, with different initial amplitudes, are shown in Fig. 16. Figure 16 shows that both large-amplitude disturbances evolve into a hairpin shape vortex, consisting of two vortical legs connected by a spanwise vortex (the head of the hairpin). The shape of the hairpin vortex depends on the geometry of the initial disturbance. Figure 17 shows the same vortical structures as in Fig. 16, but using the isosurfaces of the positive second invariant Q of the velocity gradient tensor,[26] as the method for extracting the vortical structures. Comparing Figs. 16 and 17, we can see that the shapes of the extracted vortical structures are similar. The large-amplitude initial vortical disturbance is significantly shifted from its initial position $(X = Y = Z = 0)$ during its evolution.[22] This shifting is due to the self-induced velocity (a pure nonlinear effect) and by the subsequent convection of the base flow. The detailed evolution of the nonlinear disturbances will be published in the near future.

Summary

It is demonstrated that a simple model that takes into account only the interaction between a localized vortical disturbance and a laminar uniform shear base flow is capable of reproducing the generation process and characteristics of coherent structures naturally occurring in fully developed wall-bounded turbulent shear flows. The temporal evolution of a localized vortical disturbance embedded in unbounded uniform shear laminar base flow has been studied numerically by solving the full Navier–Stokes equations. Here localized disturbance means the disturbance localized in all three dimensions and for which all dimensions are much smaller than the characteristic length scale of the base flow. We focus on the evolution of a small-amplitude initial disturbance, and only the preliminary nonlinear results are presented. The detailed evolution of the nonlinear disturbances will be published in the near future. Two different geometrical shapes of the initial disturbance (both with a Gaussian vorticity distribution) are considered: 1) Gaussian vortex (spherical vortex ring) defined by a single length scale δ, which represents the size of the localized vorticity region, and 2) toroidal vortex disturbance, defined by two length scales r_0 and δ, associated with the radius and thickness of the localized vorticity region. Note that increasing the ratio r_0/δ causes the disturbance to loose its localized character (in the streamwise and spanwise directions).

For a small-amplitude disturbance, the geometrical shape of the resulted structure is found to be sufficiently independent of the initial disturbance geometry. It consists of two flattened and elongated (in the streamwise direction) regions of concentrated vorticity, which are inclined at a small angle (<10 deg) to the base flow.

The evolution of the disturbance is governed by the transient growth mechanism. Accordingly, the induced negative velocity component grows, while the initially strong vertical component decays. Consequently, the induced disturbed velocity is mainly in the direction opposite to the base flow, which leads to the formation of an elongated (in the streamwise direction) low-speed velocity region, remindful of the streaky structures observed in turbulent boundary flows. In addition, the interaction between the negative streamwise velocity component induced by the vortical structure and base flow velocity results in the generation of local inclined shear layers of spanwise vorticity, similar to those observed in the near-wall region of turbulent and transitional flows. Note that the motion in the elongated regions of the concentrated vorticity has a strong translational component that results in a strong deviation between inclination angle of the vortical structure and vorticity vector. Consequently, in this case, the elongated vorticity regions can not be represented by a vortex filament.

The evolution process of the disturbances with different initial geometries (expressed by the length scales ratio r_0/δ) is qualitatively the same: The initial disturbance rotates around the z axis, reaches its maximum inclination angle, and then rotates in the opposite direction. The rotation process is accompanied by a significant streamwise stretching. However, the maximum inclination angle, as well as the time by which it is attained, depends strongly on the initial geometry. From the disturbed vorticity equation, one can see that the ability of the base flow shear to rotate the concentrated vorticity region depends on the gradients of the vorticity in the streamwise direction. Therefore, decreasing these gradients by increasing the length scales ratio r_0/δ results in weaker and slower rotation.

The inclination angle of the vortical structure is calculated with the aid of TED,[21] which is found to correspond well to the visual inclination angle of the vortical structure for all geometries of the initial disturbance.

The initial geometry of the disturbance has a strong effect on its transient growth. Increasing the ratio r_0/δ up to about 7 results in a more significant transient growth, which is attained at longer times. However, further increasing of the length scales ratio r_0/δ results in the reduction of the transient growth.

The necessary condition for the transient growth to take place is the presence of a spanwise structure of the initial disturbance. Note that the initial disturbance is remindful of a dipole configuration. For such dipole configurations, the radius of each leg $(\approx \delta)$ must be smaller than the distance between the centers of the two legs $(\approx 2r_0)$. Otherwise, viscous diffusion can lead to vorticity cancellation and to elimination of the vortex. On the other hand, when the spanwise separation distance is too large, the structure looses its dipole structure, which leads to decreasing vortex strength. In addition, note that when the ratio r_0/δ is increased, the gradients in the streamwise direction are decreased. Consequently, the disturbance approaches the streamwise independent state, which is known to have a more significant transient growth.[20] Indeed the results for the toroidal disturbance demonstrate the existence of such an optimal region of length scales ratios r_0/δ. In this optimal region, the spanwise separation between the two elongated vortical regions $(\approx 2r_0)$, recalculated in wall units, corresponds well to the spanwise spacing of the low-speed streaks and also to the separation distance of hairpin vortex legs observed in turbulent flows.

The results show that, at least for a limited range of parameters considered in the present study, the kinematics of the disturbance evolution depends only on its initial shape, determined by the ratio (r_0/δ), whereas its transient growth depends strongly on the Reynolds number.

Finally, the preliminary results demonstrate that a strong nonlinear initial disturbance eventually evolves into a hairpin vortex and that its shape depends on the initial disturbance geometry. The detailed investigation of the nonlinear disturbance evolution will be published in the near future.

Acknowledgment

We thank Ilia Shukhman for the fruitful discussions and collaboration during the first stages of the research and for providing us with all of the details of his analytical solution and the description of the tensor of enstrophy distribution, which allowed us to make a detailed validation of our numerical results.

References

[1]Kline, S. J., Reynolds, W. C., Schroub, F. A., and Runstadler, P. W., "The Structure of Turbulent Boundary Layers," *Journal of Fluid Mechanics*, Vol. 30, 1967, pp. 741–773.

[2]Robinson, S. K., "Coherent Motions in the Turbulent Boundary Layers," *Annual Review of Fluid Mechanics*, Vol. 23, 1991, pp. 601–639.

[3]Smith, C. R., and Walker, J. D. A., "Turbulent Wall-Layer Vortices," *Fluid Mechanics and Its Applications*, Vol. 30, 1995, pp. 235–290.

[4]Schoppa, W., and Hussain, F., "Coherent Structure Generation in Near-Wall Turbulence," *Journal of Fluid Mechanics*, Vol. 453, 2002, pp. 57–108.

[5]Blackwelder, R. F., "Analogies Between Transitional and Turbulent Boundary Layer," *Physics of Fluids*, Vol. 26, 1983, pp. 2807–2815.

[6]Breuer, K. S., and Haritonidis, J. H., "The Evolution of a Localized Disturbances in a Laminar Boundary Layer. Part 1. Weak Disturbances," *Journal of Fluid Mechanics*, Vol. 220, 1990, pp. 569–594.

[7]Breuer, K. S., and Landahl, M. T., "The Evolution of a Localized Disturbances in a Laminar Boundary Layer. Part 2. Strong Disturbances," *Journal of Fluid Mechanics*, Vol. 220, 1990, pp. 595–621.

[8]Henningson, D. S., Lundbladh, A., and Johansson, A. V., "A Mechanism for Bypass Transition from Localized Disturbances in Wall Bounded Shear Flows," *Journal of Fluid Mechanics*, Vol. 250, 1993, pp. 169–207.

[9]Acarlar, M. S., and Smith, C. R., "A Study of Hairpin Vortices in a Laminar Boundary Layer. Part 1. Hairpin Vortices Generated by a Hemisphere Protuberance," *Journal of Fluid Mechanics*, Vol. 175, 1987, pp. 1–41.

[10]Malkiel, E., Levinski, V., and Cohen, J., "The Evolution of a Localized Vortex Disturbance in External Shear Flows. Part 2. Comparison with Experiments in Rotating Shear Flows," *Journal of Fluid Mechanics*, Vol. 379, 1999, pp. 351–380.

[11]Svizher, A., and Cohen, J., "The Evolution of Hairpin Vortices in Subcritical Air Channel Flow," *Advances in Turbulence IX, Proceedings of the Ninth European Turbulence Conference*, edited by I. P. Castro, P. E. Hancock, and T. G. Thomas, International Center for Numerical Methods in Engineering, Barcelona, 2002, p. 107.

[12]Levinski, V., and Cohen, J., "The Evolution of a Localized Vortex Disturbance in External Shear Flows. Part 1. Theoretical Considerations and Preliminary Experimental Results," *Journal of Fluid Mechanics*, Vol. 289, 1995, pp. 159–177.

[13]Ellingsen, T., and Palm, E., "Stability of Linear Flow," *Physics of Fluids*, Vol. 18, 1975, pp. 487, 488.

[14]Hultgren, L. S., and Gustavsson, L. H., "Algebraic Growth of Disturbances in a Laminar Boundary Layer," *Physics of Fluids*, Vol. 24, 1981, pp. 1000–1004.

[15]Boberg, L., and Brosa, U., "Onset of Turbulence in a Pipe," *Z. Naturforschung*, Vol. 43a, 1988, p. 697.

[16]Gustavsson, L. H., "Energy Growth of Three-Dimensional Disturbances in Plane Poiseuille Flow," *Journal of Fluid Mechanics*, Vol. 224, 1991, pp. 241–260.

[17]Butler, K. M., and Farrell, B. F., "Three-Dimensional Optimal Perturbations in Viscous Shear Flow," *Physics of Fluids A*, Vol. 4, 1992, pp. 1637–1650.

[18]Reddy, S. C., and Henningson, D. S., "Energy Growth in Viscous Channel Flows," *Journal of Fluid Mechanics*, Vol. 252, 1993, pp. 209–238.

[19]Ben-Dov, G., Levinski, V., and Cohen, J., "On the Mechanism of Optimal Disturbances: The Role of a Pair of Nearly Parallel Modes," *Physics of Fluids*, Vol. 15, 2003, pp. 1961–1972.

[20]Bech, K. H., Henningson, D. S., and Henkes, R. A. W. M., "The Linear and Nonlinear Development of Localized Disturbances in Zero and Adverse Pressure Gradient Boundary-Layers," *Physics of Fluids*, Vol. 10, 1998, pp. 1405–1418.

[21]Shukhman, I. G., and Levinski, V., "Evolution of the Three-Dimensional Localized Vortices in Shear Flows. Linear Theory," *Issledovano v Rossii* [online journal], Vol. 6, 2003, URL: http://zhurnal.ape.relarn.ru/articles/2003/006.pdf [cited 15 January 2003] (in Russian).

[22]Suponitsky, V., Cohen, J., and Bar-Yoseph, P. Z, "The Development of a Localized Vortex Disturbance in Uniform Shear Flow—The Effect of the Initial Amplitude," *Proceedings of the 43rd Israel Annual Conference on Aerospace Sciences* [CD-ROM], Technion—Israel Inst. of Technology, Haifa, Israel, 2003.

[23]Suponitsky, V., Cohen, J., and Bar-Yoseph, P. Z., "The Development of a Localized Vortex Disturbance in Uniform Shear Flow—The Effect of the Initial Orientation," *Proceedings of the 29th Israel Conference on Mechanical Engineering* [CD-ROM], Technion—Israel Inst. of Technology, Haifa, Israel, 2003.

[24]"Fluent Manual," Ver. 6, Fluent, Inc., Lebanon, NH, 2002.

[25]Batchelor, G. K., *An Introduction to Fluid Dynamics*, Cambridge Univ. Press, Cambridge, England, U.K., 1967, p. 87.

[26]Hunt, J. C. R., Wray, A. A., and Moin, P., "Eddies, Stream, and Convergence Zones in Turbulent Flows," Center for Turbulence Research, Rept. CTR-S88, Stanford Univ., Stanford, CA, 1988, pp. 193–207.

C. Kaplan
Associate Editor